RESPONSE OF CONCRETE STRUCTURES TO CONFINED EXPLOSIONS OF CONDENSED CHARGES

*Matyáš Ratislav, **

Department of Concrete and Masonry Structures, Faculty of Civil Engineering,
Czech Technical University in Prague, Thakurova 7/2077, 166 29 Prague 6, Czech Republic.
matyas.ratislav@fsv.cvut.cz

ABSTRAKT

Článek se zajímá o vyčíslení zatížení a následné odezvy železobetonových konstrukcí od vnitřních a blízkých explozí kondenzovaných výbušnin. Pracuje s metodami z publikací NUREG/CR-0442 a UFC 3-340-02, které doplňuje pro rozšíření jejich rozsahu použitelnosti. Rozšíření pak umožňují posouzení použitelnosti metody pro výpočet blízkého výbuchu na blízce ohraničené konstrukce, hodnotí vliv tříštění fragmentujících prvků na odraz tlakové vlny od jejich povrchu pro vnitřní výbuch a umožňují stanovení impulzu od tlaku plynů v místnostech s více otvory. Dále je popsán zjednodušený postup vyčíslení odezvy železobetonových konstrukcí na zatížení vnitřním výbuchem. Pro řešení byly použity jednoduché inženýrské přístupy, metoda Newmark G-α a upravená metoda EC-2 pro mezní stavy použitelnosti.

KLÍČOVÁ SLOVA

Blízký výbuch • Vnitřní výbuch • Fragmentující prvek • Tlaky plynu • Betonová konstrukce

ABSTRACT

This article focuses on quantifying the loads and subsequent responses of reinforced concrete structures to confined and close-in explosions of condensed charges. It employs methods outlined in publications NUREG/CR-0442 and UFC 3-340-02, which are extended to broaden their applicability. These extensions enable the evaluation of the suitability of the method for close-in explosions on closely bounded structures, assess the impact of fragmenting of frangible elements on pressure wave reflection during internal explosions, and determine gas pressure impulses in rooms with multiple openings. Additionally, the article describes a simplified procedure for quantifying the response of reinforced concrete structures to confined explosion loading. To address these issues, simple engineering approaches, the Newmark G-α method, and a modified EC-2 method for limit state design were employed.

KEYWORDS

Close-in explosion • Confined explosion • Frangible element • Gas pressure • Concrete structure

1. INTRODUCTION

The conflict that has persisted in Ukraine over the past two years and the outbreak of the Israel-Hamas war in October 2023 serve as a reminder of the critical need for building designs that ensure the reliability of structures within the crisis infrastructure under extraordinary conditions, such as blast loads. Evaluating the structural response of concrete structures is crucial not only for building design but also for forensic analysis of past events. This is particularly relevant in the present day when conflicts are fought not only on the battlefield but also in the media.

The characteristics of loads generated by blast waves on structures depend on the chosen level of simplification, which is often determined by the explosion environment. This article discusses two types of explosions: close-in explosions and confined explosions. In the case of the former, blast waves are relatively small or comparable in magnitude to the reflecting surface, resulting in an uneven distribution of the load generated on the structure in question. For the latter, the detonation of condensed explosives occurs within a confined space, such as a building or other structure. The pressures acting on a given confinement's surface (wall or slab) are amplified by reflection from other surfaces.

2. STRUCTURAL ANALYSIS UNDER EXPLOSIVE LOADING

By the methods outlined in NUREG/CR-0442 and UFC 3-340-02 a hypothetical case study was examined. In this scenario a spherical condensed charge of Octol 70/30 with a charge weight W_{EXP} of 6.3 kg was placed in a rectangular room with two openings (the larger covered by glass and smaller without cover).

The NUREG/CR-0442 method for evaluating the response of reinforced concrete structures to close-in explosions was used to assess the damage sustained by the back wall segment (marked in blue in fig. 1). However, the source does not sufficiently express the plastic hinge radius of the damaged structure. The radius can serve as an indicator of the method's applicability to structures with supports near the explosion's 'epicentre' on the loaded structure.

---

* Supervisor: prof. Ing. Petr Štemberk, Ph.D., D.Eng.

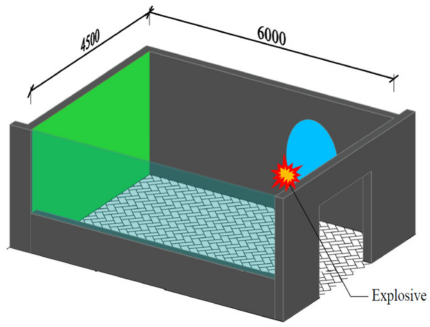

Figure 1: *Schematic axonometry of the case study.*

The evaluation of generated loads on the side wall (marked in green in fig. 1) was conducted using the method described in UFC 3-340-02 for confined explosions. However, the source does not cover the effect of fragmentation of frangible elements (e.g. glass covers) in its evaluation of blast loads caused by confined explosions. Additionally, mentioned publication does not provide a method of assessing gas pressure pulses for partially vented confinements with multiple openings.

Independent extensions have been developed to address the mentioned limitations (single opening, fragmentation of frangible elements etc.) of the methods described in NUREG/CR-0442 and UFC 3-340-02. These extensions are presented in the following paragraphs.

2.1. Close-in Explosion – Plastic Hinge Radius

NUREG/CR-0442 provides graphs with scaled units to determine the response of a wall to a close-in explosion. However, these graphs assume that the loaded surface is large enough and neglect the effect of borders and support on the local response. The method is based on the idea that the deformation of the surface can be defined by a circular plastic hinge and a deformation at the centre of the circle - the "epicentre" of the explosion (Kot et al. 1978). If the radius of the circular plastic hinge is smaller than the distance from the "epicentre" to the nearest boundary or support, it can be assumed that reasonable "first section" results can be obtained.

The presumed plastic hinge radius is the radius that corresponds to the maximum deformation value (rotation in the plastic hinge θ or the deflection in the centre δ). The deformations can be calculated as follows (Kot et al. 1978):

$$\delta = \frac{{i_T}^2}{2\, m_s F_r}, \tag{1}$$

$$\theta = arctan(\delta / x_r), \tag{2}$$

where m_s represents the mass of the surface within the plastic hinge radius x_r, F_r represents the resisting forces, and i_T is the total impulse acting on the surface within the radius calculated as: (the notation is explained in fig. 2)

$$i_{T,i} \cong \sum_{n=1}^{x_{r,i}/x_{a,step}} A_{a,n} i_{r\alpha,n}(x_{a,n}), \tag{3}$$

where $i_{r\alpha,n}$ is the reflected impulse calculated for the radius $x_{a,n}$ of the intermediary axis of the annulus.

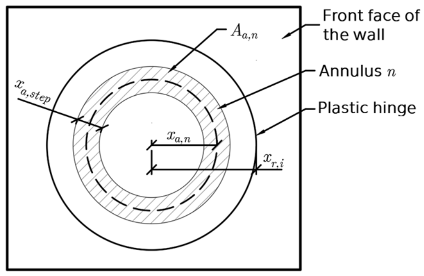

Figure 2: *Total impulse calculation - geometric relations.*

Three methods were considered to obtain this reflected impulse. The first method involves using NUREG/CR-0442 graphs (Kot et al. 1978) for shock wave parameters from free-air bursts and for reflected pressure coefficients. This method requires the calculation of a fictive scaled distance. The second method involves using more recent graphs from UFC 3-340-02 (Anon. 2008) that are similar to the first method. The third method involves using UFC 3-340-02 graphs to directly evaluate the reflected impulse. The results of different methods for the same inputs exhibited significant differences. For close-in explosions, the first approach is probably most suitable because it leads to results that closely align with the results presented in NUREG/CR-0442.

The problem was solved through iterative calculation of deformations for multiple guessed values of $x_{r,i}$. The desired radius x_r was selected based on the results, as it produced the highest deformation. It was then compared to the distance from the 'epicentre' to the nearest boundary to assess the suitability of the method used.

2.2. Reflections from Fragile Frangible Elements

According to UFC 3-340-02, when the frangible element breaks during loading, the effect of blast wave reflection from the frangible element to the adjacent surface should be reduced by creating additional venting area (Anon. 2008). This can be solved by reducing the reflection with the average fragmentation coefficient $k_{f,m} \in$ <0;1> The coefficient $k_{f,m}$ is dependent on the time evolution of the additional venting area A_{av}. The examination of this evolution should be limited to the section of the frangible element between the wall in question and the charge (see fig. 3). This is because the remaining part of the frangible element has a negligible reflection towards the wall in question (Anon. 2008). A_{av} can be created by two factors: surface deformation and fragment rotation. As the glass fragments created by blast loading are expected to be small, the contribution of rotation to the creation of A_{av} is neglected.

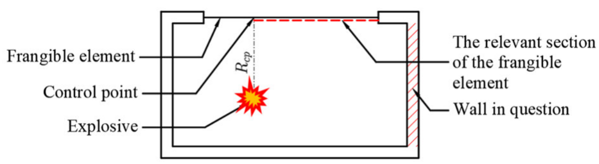

Figure 3: *Spatial arrangement schematic*

The evaluation method for $k_{f,m}$ assumes, that the primary reflections constitute the predominant source of pressure amplification on the wall in question. Therefore, the waves that reflect from multiple surfaces can be neglected. In addition, the frangible element is assumed to have little resistance to blast loading and the time to failure (fragmentation) is assumed to be zero.

Before performing the calculations, it is necessary to define the simplified shape of the deformed frangible element on which the calculation of A_{av} depends. This shape is assumed to emulate the front of the primary shock wave.

The shape of the primary shock wave was analysed in both the horizontal and vertical planes prior to impact with the glass cover in the case study setup (see fig. 4 (Li et al. 2022)). Based on the examination, a section of a cylindrical surface (see fig. 5) is considered to be the most appropriate shape simplification.

This deformed surface can be defined by the deflection u of the control point - the perpendicular projection of the point of explosion onto the plane of the frangible element – and a chord length of the cylinder section. From the geometric relations of the problem, A_{av} can be expressed as a function of the deformation at the control point u and time t, as follows:

$$A_{av} = h_{fr}\left[R_{fikt}(u,t)\,\mathrm{atan}\frac{x_{real}(t)}{R_{fikt}(u,t)-u} - x_{real}(t)\right], \tag{4}$$

where h_{fr} is the height of the frangible element,

$$x_{real}(t) = \min(x_{fr}(t); x_{\lim}), \tag{5}$$

$$R_{fikt}(u,t) = \frac{u^2 + {x_{fr}}^2}{2u}, \tag{6}$$

where x_{lim} corresponds to the length of the section, and x_u represents the distance between the control point and the intersection of the blast wave's front and the plane of the frangible element (without taking into account its deformation). This distance can be obtained from Pythagorean theorem of the distance between the explosive and the control point, and the radius of the wave front $R_{wf}(t)$.

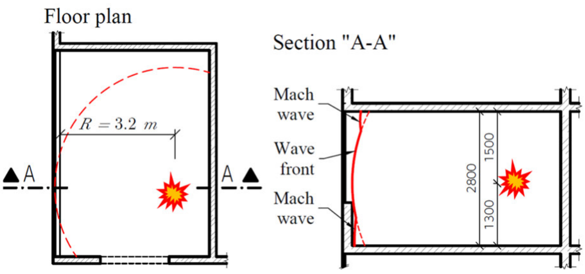

Figure 4: *Wave front shape.*

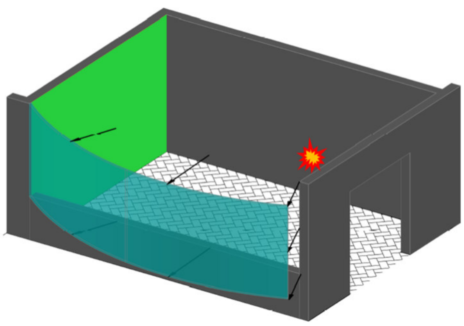

Figure 5: *Simplified shape of the deformed frangible element.*

The fragmentation coefficient k_f for a given time t and deflection of the control point u can be calculated with using following equation:

$$k_f(u,t) = \max\left[\left(1 - \frac{A_{av}(u,t)}{A_{f0}}\right)^2; 0\right], \tag{7}$$

where A_{f0} is the original (undeformed) area of the frangible elements section. Equation 7 is based on the following conditions. Firstly, the condition $A_{av} = 0 \rightarrow k_f = 1$ must be satisfied. Secondly, if $A_{av} \geq A_{f0}$, then the reflection of the wave towards the interior is negligible. This assumption is based on the principle of the wave leaking around the fragments. However, reflections can be neglected only if the clearing time t_c, which depends on the size of the fragments (Makovička et al. 2008), is less than the time taken to reach the deformation of the frangible element $A_{av} = A_{f0}$. In other words, this method is suitable for fragment sizes where $A_{av}(u(t_c),t_c) \leq A_{f0}$. Additionally, it is suggested that the reduction in reflection is more pronounced with a difference of smaller values of A_{av}, than with the same difference of larger values of A_{av}. This belief is based on the fact that the pressure gradient in the gaps is increased when the fragments are close to each other. Therefore, the drop of reflected overpressures (clearing) in front of the fragments should be increased. Equation 7 accounts for this phenomenon by squaring the expression. However, to obtain more accurate results, this engineering estimate should be refined by experiment or numerical simulation.

The average fragmentation coefficient $k_{f,m}$ can be acquired via time-stepping calculation as a weighted average of $k_{f,i-1/2}$ – the approximate average fragmentation coefficient of time step i. The weights are the reflected impulses that act on the control point during the given time step. In each time step is firstly calculated the deflection u from the linear acceleration method as (Zhou et al. 2021):

$$u_i = u_{i-1} + \dot{u}_{i-1} t_{step} + \frac{1}{6}(2\,\ddot{u}_{i-1} + \ddot{u}_i){t_{step}}^2, \tag{8}$$

where $\dot{u}$ and $\ddot{u}$ marks first (speed) and second (acceleration) derivations of the displacement u respectively. These derivations can be calculated as follows:

$$\dot{u}_i = \dot{u}_{i-1} + \frac{1}{2}(\ddot{u}_{i-1} + \ddot{u}_i)t_{step}, \tag{9}$$

$$\ddot{u}(t) = \frac{P_{cp}(t)}{\rho_{A,f}}, \tag{10}$$

where $P_{cp}(t)$ are the pressures acting on the fragments at the control point considering the effect of secondary waves. These pressures should be reduced by $k_{f,i}$ as they are also affected by the fragmentation of the frangible element. This leads to an iterative calculation of $k_{f,i}$. First the value of $k_{f,i}$ is estimated as $k_{f,i} = k_{f,i-1}$. Then, the calculation is performed using equations 8 to 10 resulting in an approximate value of u_i. This value is then used for a better estimate of $k_{f,i}$ (calculated from the equations 4 to 7). This cycle continues until the difference in u_i between subsequent iterations is less than the user selected limit.

The calculation was performed for the inputs from the case study and the results show that the effect of fragmentation is in this case neglectable: $k_{f,m} \simeq 1$. The results of the time stepping calculation are shown in following figure.

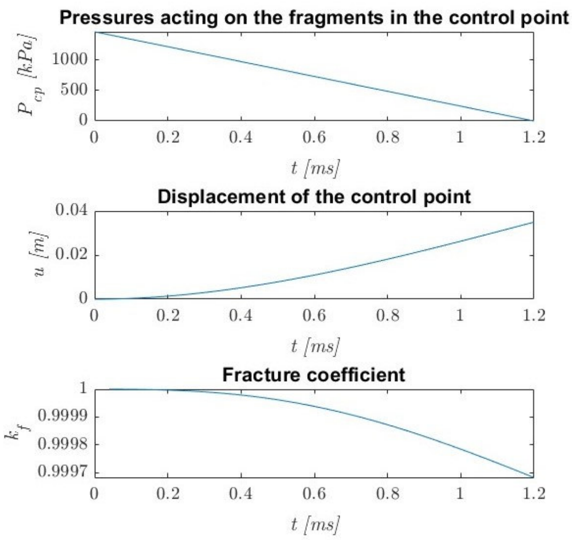

Figure 6: *Time evolution of selected quantities.*

2.3. Gas Pressures – Multiple Openings

The UFC 3-340-02 method for evaluation of gas pressures does not specify the approach for scenarios where there are multiple openings in the confinement structure. As the procedure determines the impulse of gas pressures i_g directly from its graphs, it is not easy to assess the impact of multiple openings (Anon. 2008).

The method for evaluating i_g from the UFC graphs has been developed in such a way that none of the following statements are violated during the calculation. Firstly, the impulse i_g of a room with multiple openings must always be smaller than the impulse of the same room with a single opening. Secondly, the "addition" of the effects of the openings is cumulative. And thirdly, the i_g calculated for several openings with the same characteristics (except for size) is equal to the i_g obtained for a single opening with an area equal to the sum of their areas.

First of all, the i_g must be obtained individually for each opening, without taking into account the others. Each variable, distinct for every opening, is indexed with the identification number i of the respective opening. Subsequently, the fictitious scaled vent areas, denoted as $A_{v,i,fic}/V_f^{\,2/3}$ are read for calculated gas impulses i_g from a $i_g/W_g^{\,1/3}$ to $A_v/V_f^{\,2/3}$ graph (W_g is the equivalent charge weight, A_v denotes vent area, and V_f is the volume of the confinement). The resulting actual gas pressure i_g, considering multiple openings, is then extracted from the same graph for the sum of the fictitious scaled areas.

This mentioned $i_g/W_g^{\,1/3}$ to $A_v/V_f^{\,2/3}$ graph should be obtained by interpolating UFC graphs (Anon. 2008) for parameters obtained as a weighed average of the parameters of individual openings. The weights w_i should be calculated as follows:

$$w_i = \frac{1}{\log_{10}\left(\frac{i_{g,i}}{\sqrt[3]{W_g}}\right)}. \tag{11}$$

The weighted average should be calculated on a $\log_{10}$ scale where possible (arguments are non-zero). This evaluation should be reasonably accurate for values of $A_v/V_f^{\,2/3} \leq 1$ and $\rho_{Af}/W_g^{\,1/3} \leq 19$ kg$^{2/3}$/m^2 (ρ_{Af} denotes the area density of the opening frangible cover), and should give conservative results.

The summation of the effect of vent areas than can be graphically shown in the created graph. For the case study it is as follows (O1 is the larger glass covered opening, O2 is the smaller opening without cover, both from fig. 1):

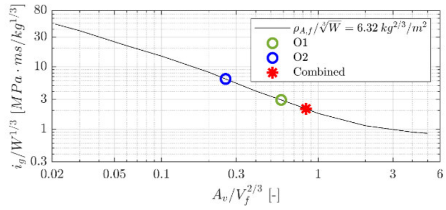

Figure 7: *interpolated $i_g/W_g^{\,1/3}$ to $A_v/V_f^{\,2/3}$ graph*

2.4. Response to Pressures form Confined Explosions

This section introduces a simplified calculation method for evaluating the response of a two-way simply supported reinforced concrete slab subjected to blast loading, where the Newmark generalised-alpha method (Erlicher et al. 2001) is applied for the dynamic calculation. However, this method has been extended for this application to take into account the non-linear behaviour of reinforced concrete. The problem is solved as a system with a single degree of freedom.

To apply the Newmark method, it was necessary to evaluate the relationship between the restoring force S and the deflection at the centre of the slab, u. This required an evaluation of the moment-curvature relationship. The procedure for calculating the limit state of serviceability from Eurocode 2-1 was used and extended to include the effects of concrete crushing and reinforcement exceeding its yield strength in tension. For simplicity the initial curvature of the wall in question was neglected, as well as the normal forces in the plane of the wall. Given these conditions the curvature κ can be calculated from the bending moment M as follows (Anon. 2019):

$$\kappa = M[(1-\zeta)C_I + \zeta C_{II}], \tag{12}$$

where ζ is the distribution coefficient calculated for a case of pure bending according to the following equation:

$$\zeta = \max\left(1 - \beta\left(\frac{M_{cr}}{M}\right)^2; 0\right), \tag{13}$$

where $\beta = 1$ for short-term loading and M_{cr} represents the bending moment which causes initial cracking. The parameter C_I can be determined as $C_I = (E_c I_{y,i})^{-1}$, where E_c is the Young's modulus of the concrete and $I_{y,i}$ is the moment of inertia of an ideal section. $I_{y,i}$ can be determined with knowledge of the concrete compression block depth x_c, which can be obtained from the equilibrium of the first moments of area on an ideal section. The value of the parameter C_{II} is dependent on the nonlinearity of the materials (method works with bilinear stress-strain diagram of both steel and concrete). It can be evaluated using the following equation:

$$C_{II} = \frac{\varepsilon_t + \varepsilon_b}{h_s} \cdot \frac{1}{M}, \tag{14}$$

where ε_t represents the strain at the top surface of the slab, ε_b at the bottom surface, and h_s denotes the height of the slab (width of a wall). The behaviour of concrete is simplified by assuming that it acts in tension until the first crack is formed, after which the concrete in tension only affects the performance of the cross-section via distribution coefficient ζ.

A programmed calculation was used to evaluate the moment-curvature relationship. For a given strain at the top surface $\varepsilon_{t,i}$, the program calculates the depths of the concrete compression block x_c for all possible combinations of the behaviour of individual parts of the cross-section. These behaviours include whether the concrete acts in tension or not, whether it is plasticized or not, and whether the reinforcement is plasticized or not. The calculation of x_c for each combination is derived from the equilibrium of forces on the cross-section. Then the conditions for the assumed behaviour in each combination are examined. If met, the moment M of the forces on the cross-section is calculated, and Equations 12 to 14 are applied. The deformations in the reinforcement and at the bottom surface can be determined, with use of similar triangles, utilizing the values of x_c and $\varepsilon_{t,i}$. This process is executed for $\varepsilon_{t,i} \in (0; \varepsilon_{c,1} >$.

The load-deflection relationship of a statically determined beam can be obtained by a simplified procedure. The beam is divided into finite sections with constant curvature defined by the derived κ to $M(f)$ relationship and the value of M evaluated for the middle of the finite section. At the ends of the beam and at the boundaries between neighbouring sections, two unknown quantities can be defined - deflection u and rotation φ, some of which can be defined by boundary conditions. For segment i, the geometric relations link the unknown quantities on both sides, resulting in a series of equations that can be used to determine the unknowns. The beam's deformation at its centre $u(M(f))$ can then be evaluated easily.

Given that the restoring force per unit area of a beam, denoted as s_b, is, in statics, equal to the loading force acting upon it, it can be stated that $s_b(u(f)) = f$. The restoring force per unit area of a two-way slab, denoted as s, can be determined as the superposition of the area restoring forces of two unit-width strips oriented perpendicular to each other, resulting in $s(u) = s_{b,x}(u) + s_{b,y}(u)$. It is worth noting that this approach does not account for the lifting of the corners of the slab.

Lastly, the relationship between the condensed restoring force S and acting on the condensed mass representing the slab, and the deflection at the centre of the slab u can be derived as follows: $S(u) = s(u)\cdot A$, where A represents the area of the slab.

For the dynamic calculation a modified Newmark G-α method was used (Erlicher et al. 2001). The damping of the system was neglected, and parameters of the calculation was set so the numerical dumping is equal to zero. The deformation in the centre of the wall in the end of the timestep was calculated as follows:

$$u_{i+1} = \frac{m\left[\frac{1-\alpha_m}{\beta}\left(\frac{u_i}{t_{step}{}^2}+\frac{\dot{u}_i}{t_{step}}+\frac{\ddot{u}_i}{2}\right)-\ddot{u}_i\right]+(1-\alpha_f)(F_{i+1}-S_{i+1})+\alpha_f(F_i-S_i)}{m\frac{1-\alpha_m}{\beta\, t_{step}{}^2}}, \qquad (15)$$

where m is the condensed mass of the wall, F denotes the loading force, t_{step} is the length of the time-step, and α and β are parameters defined by the requirement for numerical damping (Jithender & Tagir 2021).

The approach presented in this chapter can only be used until the maximal deflection u is reached, as the behaviour of the structure is not defined for a load removal. Additionally, if the ultimate load-bearing moment is exceeded, the subsequent deformation can no longer be described by this procedure.

For the wall in question the computed moment-curvature relationship of a vertical 1 m wide strip is shown in fig. 8. The result of the Newmark G-α dynamic analysis is shown in fig. 9. Based on the graphs, it can be concluded that the wall would likely remain intact after loading, but it would be severely damaged. The tension reinforcement in both directions will exceed its yield strain, and the compressed concrete will be crushed.

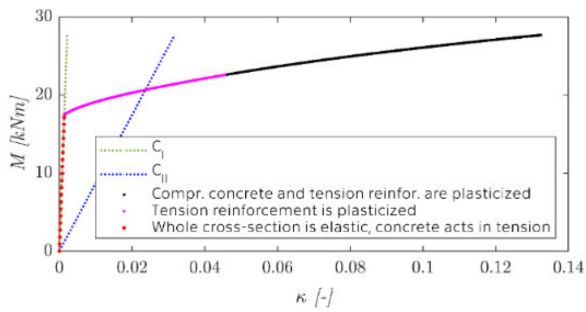

Figure 8: *Moment – curvature relationship*

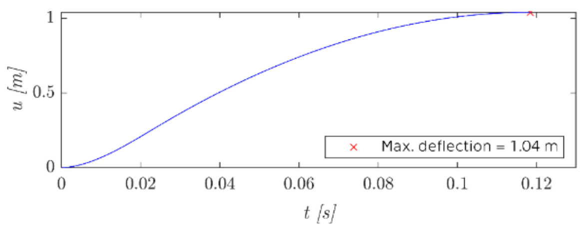

Figure 9: *Results of Newmark G-α dynamic analysis*

3. CONCLUSIONS

Limitations of the blast load assessment methods described in NUREG/CR-0442 (for close-in explosions) and UFC 3-340-02 (for confined explosions) were identified. By extending these methods, it is possible to approximately evaluate the structural response of reinforced concrete structures that are subjected to close-in explosions and have supports located relatively close to the most heavily loaded section of the structure. Additionally, it is possible to evaluate structures subjected to confined explosions with fragile, frangible elements and multiple vent openings.

The methods' extensions were applied to a complex case study. The study involved exposing a medium-sized room within a reinforced concrete structure to a 6.3 kg Octol 70/30 explosive. According to the analysis, the load-bearing structures confining the room would be severely damaged and partially disintegrated by this explosive event. Additionally, the analysis of the blast wave reflection from the frangible element shows that its fragmentation has a negligible effect in this case.

The theoretical framework presented in this thesis provides a foundation for future studies to build upon. The method for evaluating the reduction of reflected blast pressures from fragmented frangible elements could benefit from additional support or refinement through physical or numerical experiments. Furthermore, the calculation of the effect of multiple openings on the gas impulse has the potential for extension to consider heavier covers or larger openings.

ACKNOWLEDGEMENTS

The presented work has been realized within Institutional Support by Ministry of Industry and Trade of the Czech Republic and the CTU in Prague project SGS24/041/OHK1/1T/11.

References

Erlicher, S., Bonaventura, L. & Bursi, S.O., 2001. The analysis of the Generalized − α methods for non-linear dynamic problems, Università di Trento. Available at: https://hal.science/hal-00345290/document [Accessed September 19, 2023].

Jithender, T. & Tagir, I., 2021. Lecture 4: Generalized-Alpha Method / Newmark Method. YouTube. Available at: https://www.youtube.com/watch?v=wUsTSm-DY1g&t=290s&ab_channel=ComputationalDynamics [Accessed November 7, 2023].

Kot, C.A. et al., 1978. Nureg/CR-0442: Effects of air blast on power plant structures and components, Argonne National Lab., IL (USA). Available at: https://inis.iaea.org/collection/NCLCollectionStore/_Public/10/448/10448846.pdf?r=1 [Accessed September 19, 2023].

Li, X.-long et al., 2022. Numerical simulations of trajectories of shock wave triple points in near-ground explosions of TNT charges. Energetic Materials Frontiers, 3(2), pp.61-67. Available at: https://www.sciencedirect.com/science/article/pii/S2666647222000331 [Accessed March 18, 2024].

Makovička, D., Janovský, B. & Černín, M., 2008. Příručka protivýbuchové ochrany staveb, Praha: Česká technika - nakladatelství ČVUT v Praze. Available at: http://www.makovicka.cz/data/S/U/t/2008-pvoch-cz.pdf [Accessed March 18, 2024].

Zhou, Z. et al., 2021. Fundamentals of structural dynamics, Cambridge, MA: Elsevier. Available at: https://www.sciencedirect.com/topics/engineering/linear-acceleration-method [Accessed March 18, 2024].

Anon., 2008. UFC 3-340-02 Structures to Resist the Effects of Accidental Explosions, U.S. Army Corps of Engineers. Available at: https://www.wbdg.org/FFC/DOD/UFC/ARCHIVES/ufc_3_340_02.pdf [Accessed September 19, 2023].

Anon., 2019. Eurokód 2: Navrhování betonových konstrukcí - Část 1-1: Obecná pravidla a pravidla pro pozemní stavby.